

# Suspended sediment transport in the German Wadden Sea—seasonal variations and extreme events

Alexander Bartholomä · Adam Kubicki ·  
Thomas H. Badewien · Burghard W. Flemming

Received: 12 November 2008 / Accepted: 8 March 2009  
© Springer-Verlag 2009

**Abstract** The German Wadden Sea (southern North Sea) sediments are composed of both cohesive and non-cohesive deposits. The spatial distribution patterns are mainly driven by wind-induced waves and tidal currents. Transport intensity and duration depend on the hydrodynamic conditions, which vary over time. In this paper, the transport of suspended sediment was investigated on seasonal, tidal and hourly time scales in the back-barrier system of Spiekeroog Island. Long- and short-term data of fair weather periods and two storm events were investigated based on stationary and mobile measurements of currents and waves by Acoustic Doppler Current Profiler (ADCP), in situ particle size and suspended sediment concentration (SSC) measurements by laser in situ scattering and transmissometry (LISST) as well as wind records. The ADCP backscatter intensities were calibrated by means of LISST volume concentration data in order to quantify longer term SSCs and fluxes in the back-barrier system. Values up to  $120 \text{ mg l}^{-1}$  were recorded, but concentrations more commonly were below  $60 \text{ mg l}^{-1}$ . The long-term results confirm former observations of a balanced budget during low-energy (fair weather) conditions in the study area. In general, SSCs were higher during spring tides than during neap tides. The data also clearly show the remobilisation of sediment by

tidal current entrainment. The records include two severe storm events, “Britta” (1st November 2006) and “Kyrill” (18th January 2007). The data reveal very complex temporal flow and transport patterns. During both storm events, the export of material was mainly controlled by the interaction of wind, waves and tidal phase. The typical ebb-dominance occurring during fair-weather conditions was temporarily neutralised and even reversed to a flood-dominated situation. During “Kyrill”, the wind and high-waves setup in conjunction with the tidal phase was even able to compress the duration of two successive ebb cycles by over 70%. Although SSCs increased during both storms and higher turbulence lifted particle clouds upwards, an export of suspended matter towards the North Sea was only observed under the conditions taking place during “Britta”. Such fluxes, however, are currently still difficult to quantify because the backscatter intensity during high energy events includes a substantial amount of noise produced by the high turbulence, especially near the water surface.

**Keywords** Wadden Sea · SPM transport · Storm events · Time series · Waves · Currents · Tidal system · SSC · ADCP · LISST

---

Responsible Editor: Jürgen Rullkötter

---

A. Bartholomä (✉) · A. Kubicki · B. W. Flemming  
Department of Marine Science, Senckenberg Institute,  
Suedstrand 40,  
26382 Wilhelmshaven, Germany  
e-mail: abartholomae@senckenberg.de

T. H. Badewien  
Institute of Physics, University of Oldenburg,  
Carl-von-Ossietzky-Str. 8-11,  
26129 Oldenburg, Germany

## 1 Introduction

The spatial distribution pattern of German Wadden Sea sediments is mainly driven by wind-induced waves and tidal currents. In the back-barrier area, grain sizes range from clay to medium sand (see e.g. Flemming and Ziegler 1995). The general sediment distribution pattern shows a relatively steady shore-parallel zonation, but seasonally, grain-size composition and spatial patterns show significant variations (e.g. Mai and Bartholomä 2000; Bartholomä and

Flemming 2007; Chang et al. 2007). It was postulated by Flemming (2002) that higher water levels due to sea-level rise will produce an increasing sediment deficit in the tidal basins and that the expected morphodynamic response will result in an accelerated shoreward migration of the barrier islands. As a consequence, the increase in hydrodynamic energy should result in an increasing export of fine-grained sediments towards the North Sea. In general, sediment flux and model studies so far did not show any significant export or import of sediment out of or into the tidal basins during calm-weather conditions (Santamarina Cuneo and Flemming 2000; Stanev et al. 2007). It was found that non-cohesive coarse silt-fine sand particles and aggregates are transported in suspension during all weather conditions, whereas sand transport is restricted to high energy conditions when wind speeds exceed 6 Bft and wave heights reach 1 m or more along the Wadden Sea coast (Santamarina Cuneo and Flemming 2000).

The spatial range of transport is mainly controlled by the tidal currents. During the flood phase, water from the open sea enters the tidal inlet with speeds  $>1 \text{ m s}^{-1}$ . In the back-barrier tidal basins, the flood water mixes with water from the preceding ebb phase. During the ebb phase, water enriched in suspended sediment flows out at generally higher flow velocities than during the flood phase, and the tidal basins are therefore characterised as being ebb-dominated (Stanev et al. 2003a, b). These tide-related processes play an important role in controlling the sediment budget of the tidal basins. In dependence of the seasonal variations in wind, waves and water level changes, the suspended sediment varies in its grain-size composition and concentration. These periodical variations can be temporarily overprinted by the effects of superimposed extreme high-energy events, which can evidently change the sediment budget temporally or even permanently (e.g. Bartholdy and Aagard 2001; Lumborg and Pejrup 2005; Talke and Stacey 2008; Badewien et al. 2009).

The spatial distribution of fine-grained sediment deposits is well known from many locations of the Wadden Sea (e.g. Pejrup 1988; Edolvang and Austen 1997; de Haas and Eisma 1993; Xu 2000; Chang et al. 2006). General aspects of the hydrodynamic processes involved have already been discussed in several papers on hydrological modelling (e.g. Stanev et al. 2003a, b, 2006). However, continuous time-series and event-related field data are still needed to understand the suspended sediment budget and to better validate and parameterise sediment transport models. To compensate this lack of in situ information, field measurements were carried out in the back-barrier tidal basin of Spiekeroog Island (East Frisian coast, Germany) on different time scales, both at stationary sites and in mobile configurations. The measuring programme focused on the identification of typical seasonal conditions and extreme

events to work out mean suspended sediment concentrations (SSC), in situ particle sizes and the influence of local hydrodynamic conditions.

## 2 Physical setting and study site

The study site is situated south of Spiekeroog in the German Wadden Sea, southern North Sea (Fig. 1). Spiekeroog is one of the barrier islands of the Wadden Sea stretching from The Netherlands in the west to Denmark in the northeast. The investigated area itself is located in the Otzum Inlet, the main tidal channel linking the tidal catchment with the North Sea. The tide is semidiurnal with a mean tidal range of 2.8 m, thus belonging to the upper mesotidal regime in the classification of Hayes (1979). The water exchange is characterised by a tidal phase asymmetry (Fitzgerald and Penland 1987), the ebbing tide being of shorter duration and slightly higher velocity than the flooding tide. Former point measurements show maximum current velocities of up to  $1.3 \text{ m s}^{-1}$  during calm weather conditions in the main channels (Davis and Flemming 1991; Santamarina Cuneo 2000) and up to  $0.3 \text{ m s}^{-1}$  on the tidal flats (Bartholomä 1993). The maximum water exchange during spring tide amounts to about  $140 \times 10^6 \text{ m}^3$  per ebb/flood and the residual water body in the Otzum tidal basin at low tide amounts to about 25% of this volume.

## 3 Materials and methods

Hourly or daily stationary field measurements were carried out on several campaigns from the research vessel “Senckenberg” along different locations in the Otzum Inlet. Longer time series including seasonal variations and extreme events were registered at the measurements pile station (for details, see Reuter et al. 2009) where an up-looking Acoustic Doppler Current Profiler (ADCP) collected data from October 2006 to June 2007. The pile is positioned along the northern margin of the Otzum channel at the southwestern end of Spiekeroog Island (pile in Fig. 1). Short-term current patterns along a tidal channel cross-section over individual tidal cycles were acquired with a small motorboat (transect in Fig. 1).

Time series measurements from R/V “Senckenberg” included in situ particle-size data from a laser particle sizer [laser in situ scattering and transmissometry (LISST) 100ST], water samples as well as current velocities and directions from an ADCP (RDI-Teledyne Broadband, 1.2 MHz, 0.25 m bin size and 0.5 m blank spaces in the near and far ranges) operating in the down-looking bottom-tracking mode. The in situ particle size mostly reflects aggregated very fine silt particles forming flocs (Chang et

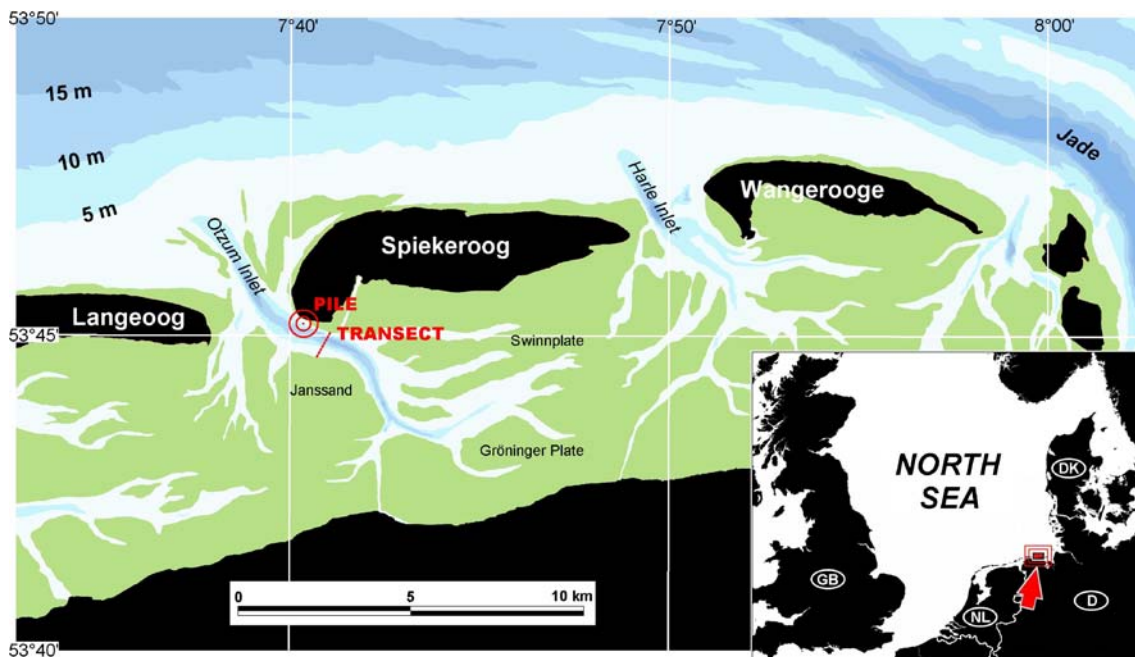


**Fig. 1** Study sites on the topographic map of the back barrier tidal flats (inter-tidal section marked *green*) of Spiekeroog Island. The *red dot* shows the position of the research pile in the main drainage channel Otzum Inlet and the *red line* represents an approximate

transect orientation for the across channel mobile ADCP profiles. The stationary vessel measurements were taken at the southwestern end of the transect

al. 2007). Stationary current and wave measurements were done with an ADCP (RDI-Teledyne Workhorse, 1.2 MHz, 0.25 m bin size and corresponding 0.5 m blanks) installed near the channel bed 8 m away from the pile looking upward. The sensors were located about 0.75 m above the channel bed, and therefore, a significant part of the near-bed suspension information is missing.

The LISST 100 (Sequoia Scientific, Inc., USA) continually scans small volumes of water and records laser scattering at 32 angles, which are subsequently converted into particle-size distributions. Additionally, water depth, temperature and the overall optical transmission are recorded.

Particle distributions can be mathematically converted into volume concentrations given in units of millilitre per litre, which the manufacturer considers a relatively “reliable” quantification of sediment in suspension (Agrawal and Pottsmith 2000). However, the uncertainty in particle density may cause errors of 10% (Fettweis 2008), whereas the lack of knowledge of particle shapes will produce even greater errors (Agrawal et al. 2008). To estimate the density of suspended matter, the volume concentrations given by the LISST 100 were compared with those obtained from water samples. For this purpose, volumes of seawater between 72 and 277 l were pumped simultaneously at a water depth of about 3 m. Particle volume concentrations were compared with grain size analysis of collected sediments. These were obtained after centrifuging the water samples. In addition, equations provided by Agrawal and

Pottsmith (2000), which simplify SSC calculations in correlation with optical transmission values, were utilised.

The ADCP simultaneously emits four acoustic pulses into the water column and records their backscatter from suspended organic and inorganic particles as well as from air bubbles. The 1.2 MHz system is limited to depths up to 25 m registering in cells 0.25 m thick. The relatively strong signals backscattered from the seabed in the down-looking configuration allow bottom tracking and hence water depth determination. In the up-looking configuration, on the other hand, ADCPs fitted additionally with pressure sensors are able to track the water surface and thereby analyse wave spectra. Moreover, the amount of scatterers in the water controls the strength of the returning signals to the ADCP sensors. In this way the backscatter intensity carries information about SSC, which can then be estimated after appropriate calibration. A number of approaches have been proposed for the conversion of ADCP signals into SSC values based on signal calibration against simultaneous water sampling (e.g. Kawanisi and Yokosi 1997; Holdaway et al. 1999; Fugate and Friedrichs 2002; Nikora and Goring 2002; Voulgaris and Meyers 2004; Hoitink and Hoekstra 2005; Merkelbach 2006; Trevethan et al. 2007). Experiments performed in the laboratory usually produced good correlations, whereas unpredictable dynamics of the natural system still limits the accuracy of conversions of in situ data sets into SSC.

In this paper, we used a LISST device for calibrating the ADCP signals. Good quality in situ data sets for both

devices were acquired simultaneously in a 2-day measuring campaign (27–28 July 2004). SSC values recorded by LISST were compared with ADCP backscatter signal strength from 7475 corresponding depth cells (Fig. 2c). Samples analysed from depths larger than 1 m are shown in dark green, those near the surface in light green. The scatter plot shows that the largest discrepancies are observed in the near-surface volume. Here, the higher concentrations represent the superimposition of the signals produced by particle scatters and noise produced by turbulence and air bubbles. Unfortunately, the ADCP working principle does not allow to filter out these noise values. Because the near-surface volume also contains significant information on suspended sediment, the statistically best-fitting curve was obtained for all investigated sample points, in spite of the superimposed noise. Until a method for the elimination of noise components is available, Eq. 1 is currently treated as a universal algorithm for direct conversion of ADCP signals into SSC values.

$$C = 0.2382 e^{0.0437BS} \tag{1}$$

$C$  is SSC given in milligram per litre and  $BS$  is acoustic backscatter given in dB. This equation was subsequently also applied to the data from the pile-mounted upward-looking ADCP.

## 4 Results

### 4.1 Volume and mass concentration (ADCP and LISST)

The data set of an almost 21-h long time period on 27–28 July 2004 recorded maximum backscatter values of nearly

100 dB and SSC values reaching  $35 \text{ mg l}^{-1}$  for near-surface pixels (Fig. 2). The regression curve with a correlation coefficient of  $R=0.67$  is considered valid only for concentrations of less than  $25 \text{ mg l}^{-1}$ . Because of this limitation, the absolute concentrations in suspended matter are presumably underestimated.

In contrast to single-point measurements of the LISST system, the ADCP data covers the entire water column. LISST SSC values were also correlated with SSC data of water pump samples with time-averaged volumes of 230 l (Fig. 3, red dots). The good fit between these two data sets shows maximum SSC of up to almost  $17 \text{ mg l}^{-1}$  in the water samples and exceeding  $50 \text{ mg l}^{-1}$  in the ADCP data set. These values are compatible with the observations at low energy conditions in the case study of Santamarina Cuneo (2000). However, at high energy conditions, the concentrations of coarser grain sizes differ significantly in the two studies. The relative differences reflect the wider spectrum of particle sizes and concentrations at the different time scales characterising the two studies.

### 4.2 In situ floc sizes and SSC variability on different time scales

#### 4.2.1 Short-term period: tidal cycles

Floc sizes and SSC are strongly controlled by the variable energy conditions in the course of individual tidal cycles. Maximum concentrations exceeding  $30 \text{ mg l}^{-1}$  are observed during the initial ebb phase after slack high water, whereas during flooding, they only reach  $20 \text{ mg l}^{-1}$ . At slack low water, SSC falls below  $10 \text{ mg l}^{-1}$ . At the same time, the floc size reaches its highest values exceeding  $400 \mu\text{m}$ , whereas

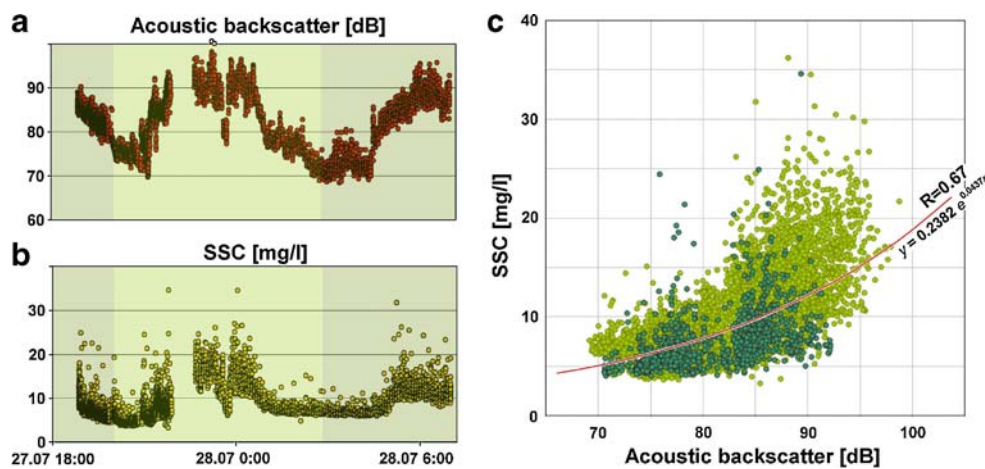


**Fig. 2** **a** Acoustic backscatter recorded during a 21-h experiment on 27–28 July 2004; **b** suspended sediment concentration (SSC values) derived from LISST volume concentration during the same experiment; **c** correlation of acoustic backscatter vs SSC values selected from corresponding water depths. The plot contains 7475 sample

pixels collected in the vicinity of the research pile. Note a significant deviation from the best-fitting curve, especially for sample points located in the near-surface, 1 m deep volume (light green), which is fairly characteristic for turbulent environments

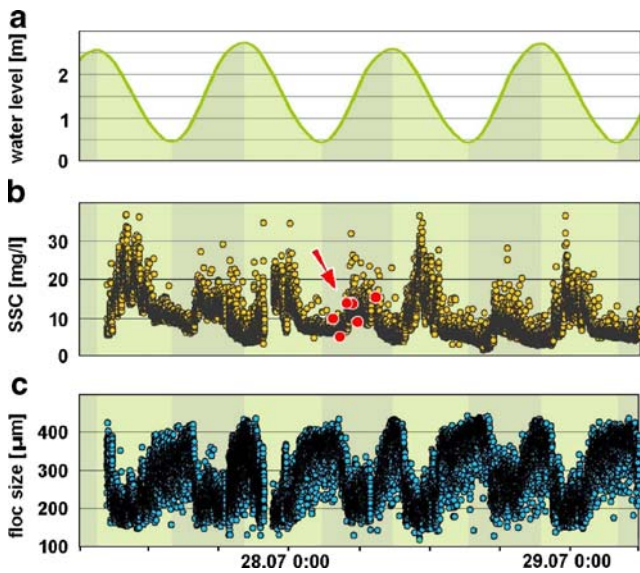


**Fig. 3** Suspended sediment concentration measurements (b) and in situ floc sizes (c) over tidal cycles from 27 to 29 July 2004 (a). The red dots on the SSC plots mark the concentrations of in situ pump-water samples

during the flooding and ebbing tides, the floc size decreases to below 200 µm (Fig. 3). In general the mean floc size ranges from 100 to 305 µm depending on hydrodynamic conditions (Table 1).

Floc sizes and SSC are strongly limited by the tidal flow velocity (Fig. 4). Above a critical velocity of about 0.8 m s<sup>-1</sup> the SSC remains stable, and transport conditions appear to arrive at a “steady state” for the floc sizes at both ends of the energy gradient during tidal cycles. The floc sizes vary between 350 µm for low current speed to 250 µm for maximum current speed.

This example from May 2002 demonstrates that, during the tidal flow phase, all easily erodible material is resuspended after slack water and that more consolidated cohesive sediments or sand remain on the bed. The quasi-stable floc size at high flow velocities appears to be resistant to the current shear, probably due to high internal binding forces.

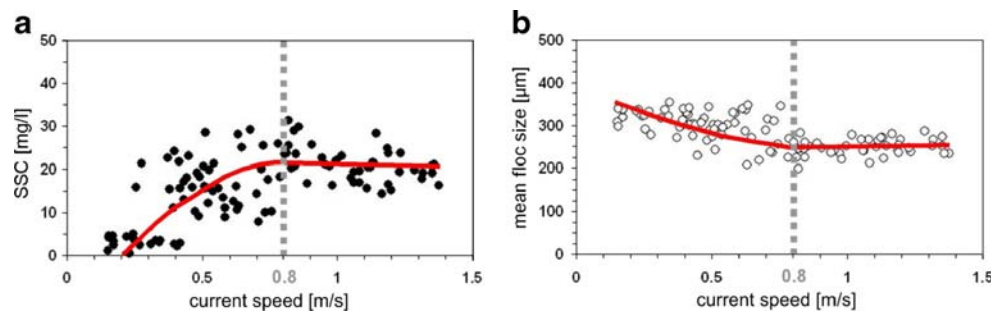
Apart from the current velocity, the particle remobilisation in the tidal basin strongly depends on wave action. Even under relatively quiet weather conditions, small waves in shallow water are already able to entrain loose flocs and aggregates. For instance, the occurrence of small waves during the flooding/ebbing tide will generate higher

**Table 1** LISST and water sampling results of SSC and mean floc sizes from stationary vessel measurements in the vicinity of the pile

	DATE	LISST LONGEST CONTINUOUS DURATION [h]	FLOC SIZE			CALCULATED SSC			WATER SAMPLES	MEASURED SSC	
			MIN [µm]	MAX [µm]	MEAN [µm]	MIN [mg/l]	MAX [mg/l]	MEAN [mg/l]	AMOUNT	MIN [mg/l]	MAX [mg/l]
W	05-06.XII.2001	10	57	239	122	34	49	41	3	30.5	48.3
W	08-09.I.2002	17	74	307	149	2	43	25	1	11.7	11.7
W	07.II.2002	0.2	34	120	105	30	54	48	2	41.8	65.5
S	26-27.III.2002	6	71	289	164	12	48	37	-	-	-
S	08.V.2002	7	197	346	293	12	47	36	8	5.8	27.2
S	03-04.VI.2002	17	169	387	279	13	41	21	2	1.5	2.9
W	12-13.XI.2002	7	149	360	203	5	51	32	11	12	51.9
W	20-21.I.2003	4	119	272	194	3	49	34	-	-	-
W	17-20.II.2003	9	70	295	190	1	36	21	-	-	-
S	13-14.V.2003	23	62	397	237	0	33	12	-	-	-
S	17-18.VI.2003	20	31	418	147	0.3	16	8	-	-	-
S	22-23.VII.2003	19	68	360	151	0.1	8	3	-	-	-
S	26-28.VIII.2003	9	32	277	100	0	9	3	-	-	-
W	29.X.2003	1	185	331	213	1	10	6	6	8.7	54.3
S	8.VI.2004	4.5	88	375	239	8	37	18	-	-	-
S	27-29.VII.2004	46	117	433	305	6	36	9	6	5.5	16.7
S	17-21.IX.2004	101	121	359	228	15	35	25	-	-	-
W	15-16.XI.2004	15	79	365	217	22	38	32	8	64.2	120.5

Measurements were divided into winter (W) and summer (S); and according to the Moon phase into neap (in blue) and spring tide ones. Arithmetic mean values are given for all recorded data samples

**Fig. 4** **a** Correlation of suspended sediment concentration (SSC values) vs tidal current speed and **b** mean floc sizes vs current speed. Note changes in trend for current speeds larger than 0.8 m/s. Data from May 2002: water depth 2 m, 5.5 h of data



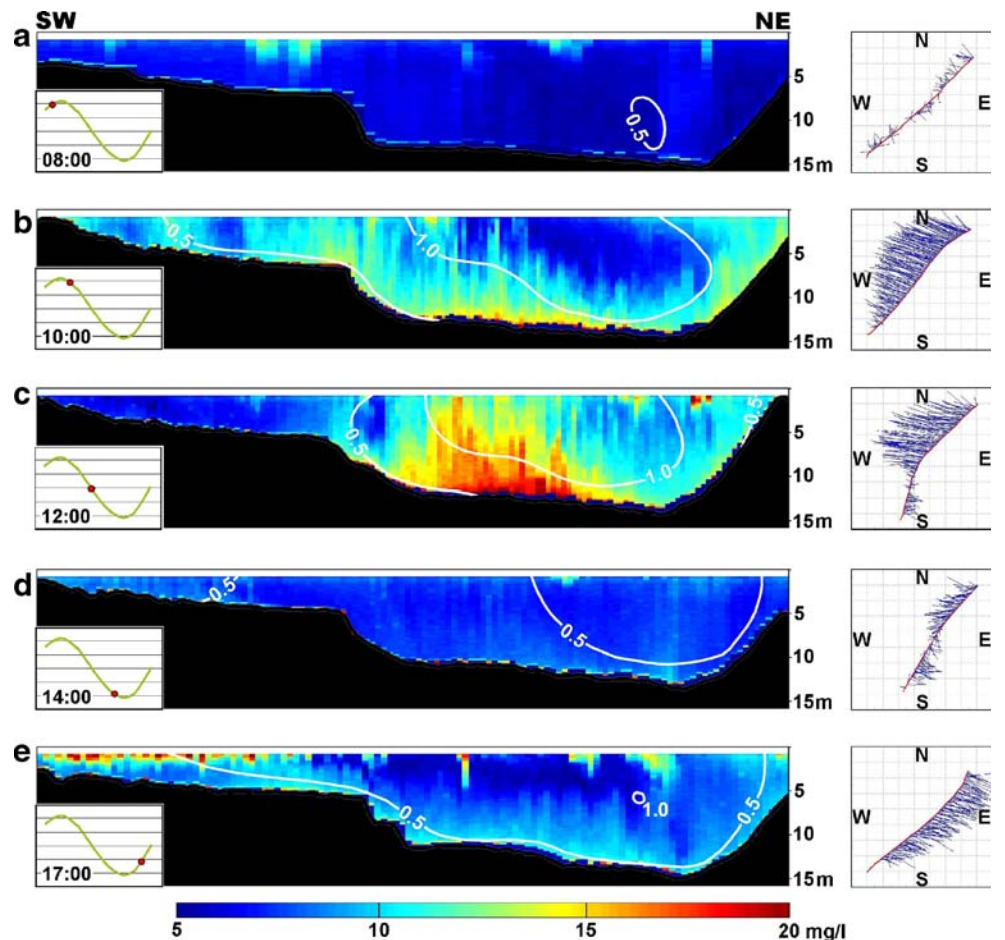
turbulence. This additional wave impact of course depends on the water depth as well as current directions and hence varies over the tidal cycle. This means that, mostly, the tidal flats and the shallower parts of tidal channels are affected.

The duration of resuspension is time and energy limited. ADCP measurements over individual tidal cycles along cross-channel transects by means of a ship-mounted instrument track the sediment transport characteristics within the channel (Fig. 5).

During slack water at 08:00 hours (Fig. 5a), SSC distribution in the water column is quite uniform at 7–8 mg l<sup>-1</sup>.

At 10:00 hours, when the ebbing flow accelerates, a cloud of sediment with a SSC close to 15 mg l<sup>-1</sup> is being lifted from the bed of the channel. At 12:00 hours, when the current is fully developed, the sediment cloud reaches the surface, and SSC values close to the bed now exceed 20 mg l<sup>-1</sup>. Two hours later at 14:00 hours, just before slack water, concentrations are again uniformly distributed at concentrations close to 10 mg l<sup>-1</sup>. During the onset of the subsequent flooding phase (Fig. 5e), the overall SSC again rises but now shows a pattern different from that during the initial ebbing phase. The spatial distinction of these

**Fig. 5** **a–e** Vessel-mounted ADCP transects during a 9-h experiment on 28 July 2004 (see Fig. 1 for location). SSC scale is common for all images. Current speed isolines (in white) are given in metre per second. The tidal phase is shown by red dots in left subwindows, whereas velocity vectors are presented in blue on the right side. A true ship path is delineated there in red over a 100-m grid and is geographically aligned. Note lifting of sediment from the seabed during increasing current speeds



different SSC patterns is caused by the bidirectional flow in the course of a tidal cycle (Santamarina Cueno and Flemming 2000).

4.2.2 Medium-term period: spring–neap cycles

With the changing tidal range from neap tide to spring tide, the ebb dominance is emphasised (Fig. 6). Increased water level and current speed results in higher SSC values. During spring tide, depth-integrated concentrations exceeding  $15 \text{ mg l}^{-1}$  are observed, whereas during neap tide, the values barely reach  $12 \text{ mg l}^{-1}$ . The flood flow, on the other hand, is not significantly affected by the moon phase and depth-averaged SSCs range between 10 and  $12 \text{ mg l}^{-1}$ .

4.2.3 Longer term periods: seasonal variations

Over longer time intervals, e.g. several seasons, one would intuitively expect to observe significant changes in SSCs and their distribution in the water column. However, the daily to two-daily vessel-based stationary time-series measurements of in situ particle sizes and water sample analyses in the period from December 2001 to November 2004 do not show a significant seasonal dependence of SSC variations (Table 1). Only in November 2004, clearly higher concentrations of up to  $120 \text{ mg l}^{-1}$  were recorded.

In contrast to the almost steady SSC values, the floc size does vary over the seasons. The in situ particle-size measurements of the LISST showed a maximum floc size of  $433 \mu\text{m}$  in July 2004, a value that appears to be limited by the hydrodynamics of the study area or by device sensitivity. The minimum and maximum floc sizes during

the winter period reach 32 and  $217 \mu\text{m}$ , respectively, whereas for the summer period values between 31 and  $433 \mu\text{m}$  were recorded (Table 1).

4.2.4 Extreme events: storms “Britta” and “Kyrill”

During the recording period of the pile-mounted ADCP, several significant storm events were captured. On 1st November 2006 storm “Britta” crossed the German North Sea, inducing rarely recorded high-water levels of 3.3 m above the mean sea level. At that time, most of the small harbours along the East Frisian coast were submerged. The storm surge and wave activity resulted in damage to harbour constructions and vessels. Storm “Britta” occurred during the flood phase with waves from westerly directions. The superimposition of the flood flow and waves resulted in higher backscatter intensity, indicating greater turbulence and intensified resuspension over the entire water column (Fig. 7a). During this high-wave period, substantial suspended sediment clouds were lifted from the channel bed, concentrations at 8 m above the bed reaching over  $15 \text{ mg l}^{-1}$ . Depth-averaged SSC values considerably exceeded  $15 \text{ mg l}^{-1}$  during this surge as compared to  $10 \text{ mg l}^{-1}$  observed during pre-storm flood phases (Fig. 7b), but it must be remembered that these values are underestimations due to the lack of near-bed backscatter information. The flood current speeded up to  $1.8 \text{ m s}^{-1}$ , and the recorded significant wave height exceeded 1.25 m.

The situation changed rapidly during the next slack water when the wind direction rotated quasi-simultaneously with the upcoming slack water. With a significant wave height of still almost 1 m, the change in wind direction

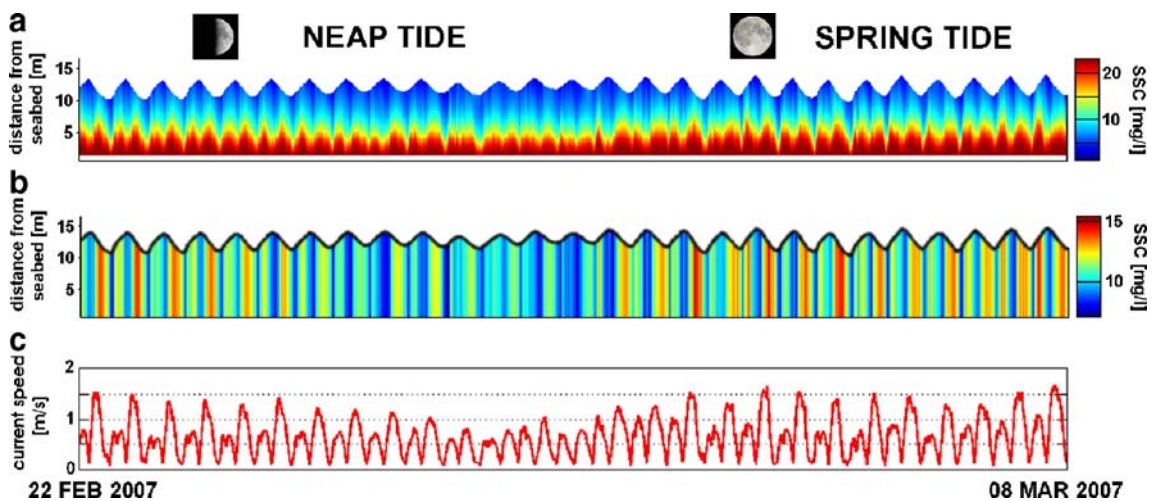
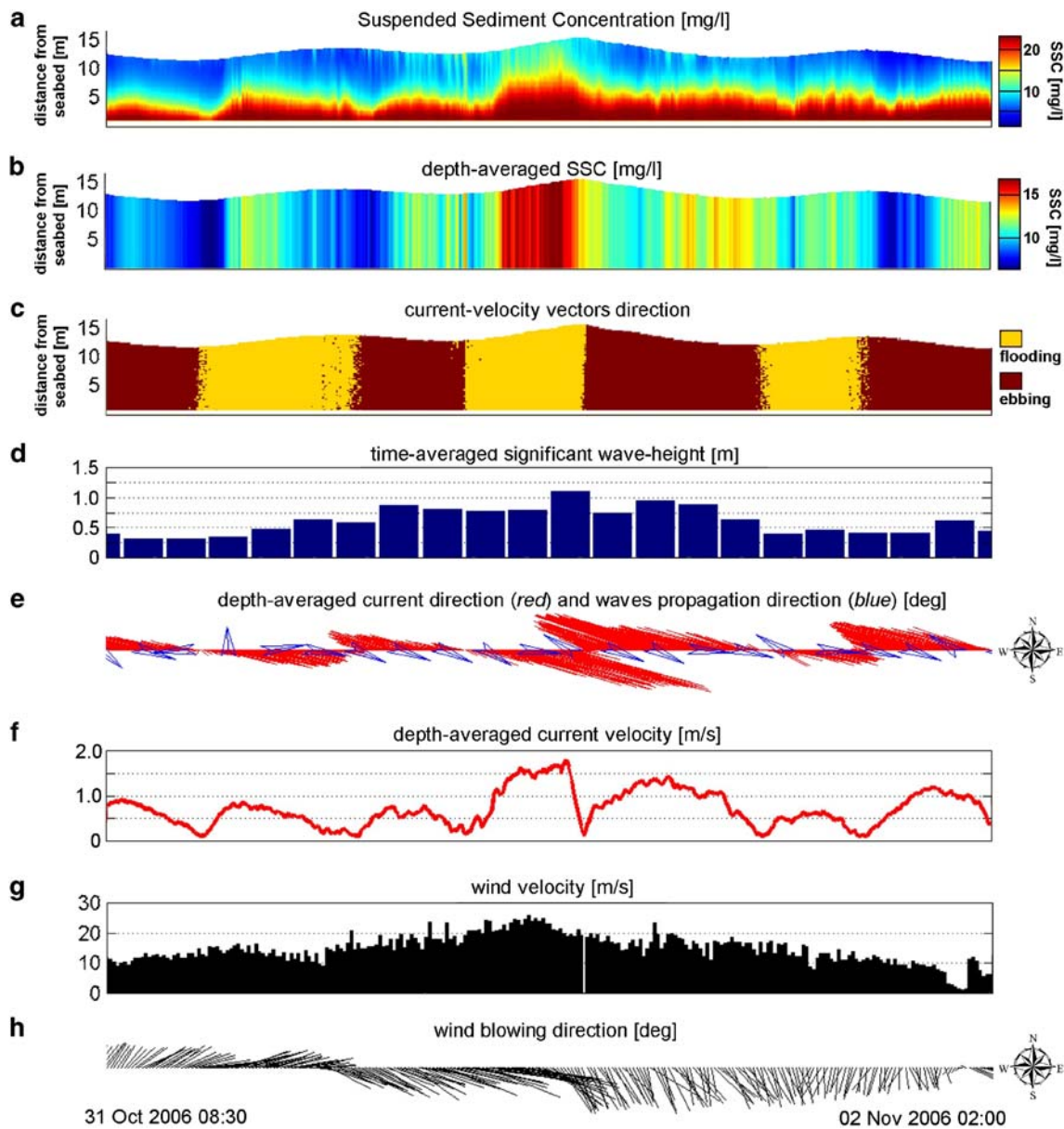


Fig. 6 a SSC values at different water depths and b depth-integrated SSC values during calm weather conditions between 22nd February and 8th March 2007. Note the difference of concentration during neap- and spring-tide periods observed as the increase of SSC values

in the centre and upper section of the water column. The depth-integrated SSCs are most probably underestimated due to lack of near-bed information



**Fig. 7** Storm surge “Britta” on 1st November 2006 shown as **a** backscatter-related SSC; **b** depth-averaged backscatter-related SSC; **c** water flow direction; **d** significant wave height; **e** depth-integrated

flow direction and wave propagation direction; **f** depth-averaged flow velocity; **g** wind velocity; and **h** wind blowing direction. The maximum storm intensity took place during the flood phase

from WNW to NNW prolonged the next ebb phase. In spite of this and the fact that the ebb current reached a peak flow velocity of nearly  $1.5 \text{ m s}^{-1}$ , the SSC decreased rapidly.

Almost 3 months later, on 18th January 2007, the storm “Kyrill” passed the German North Sea coast. In contrast to storm “Britta”, this storm hit the coast during the ebbing tide (Fig. 8). In spite of this, the wind was nevertheless able to push substantial amounts of water into the back-barrier basin against the ebb current. This is well documented in the water-level record as well as in the depth-averaged current speed and direction. The subsequent “unusually”

extended flood period was characterised by waves with significant heights just below 1 m (Fig. 8).

In this specific situation, the change in wind direction and tidal current speed squeezed the ebb phase to nearly 30% of its normal duration. In consequence, the ebb flow speed was reduced to less than  $0.5 \text{ m s}^{-1}$ , i.e. less the half of the usual speed (black circle Fig. 8f). This effect also influenced the next flood phase, which was prolonged by around 20% of its normal duration. However, with the rapid change in wind direction and decelerating wind speed, the system was “reset” in a single ebb phase, which was

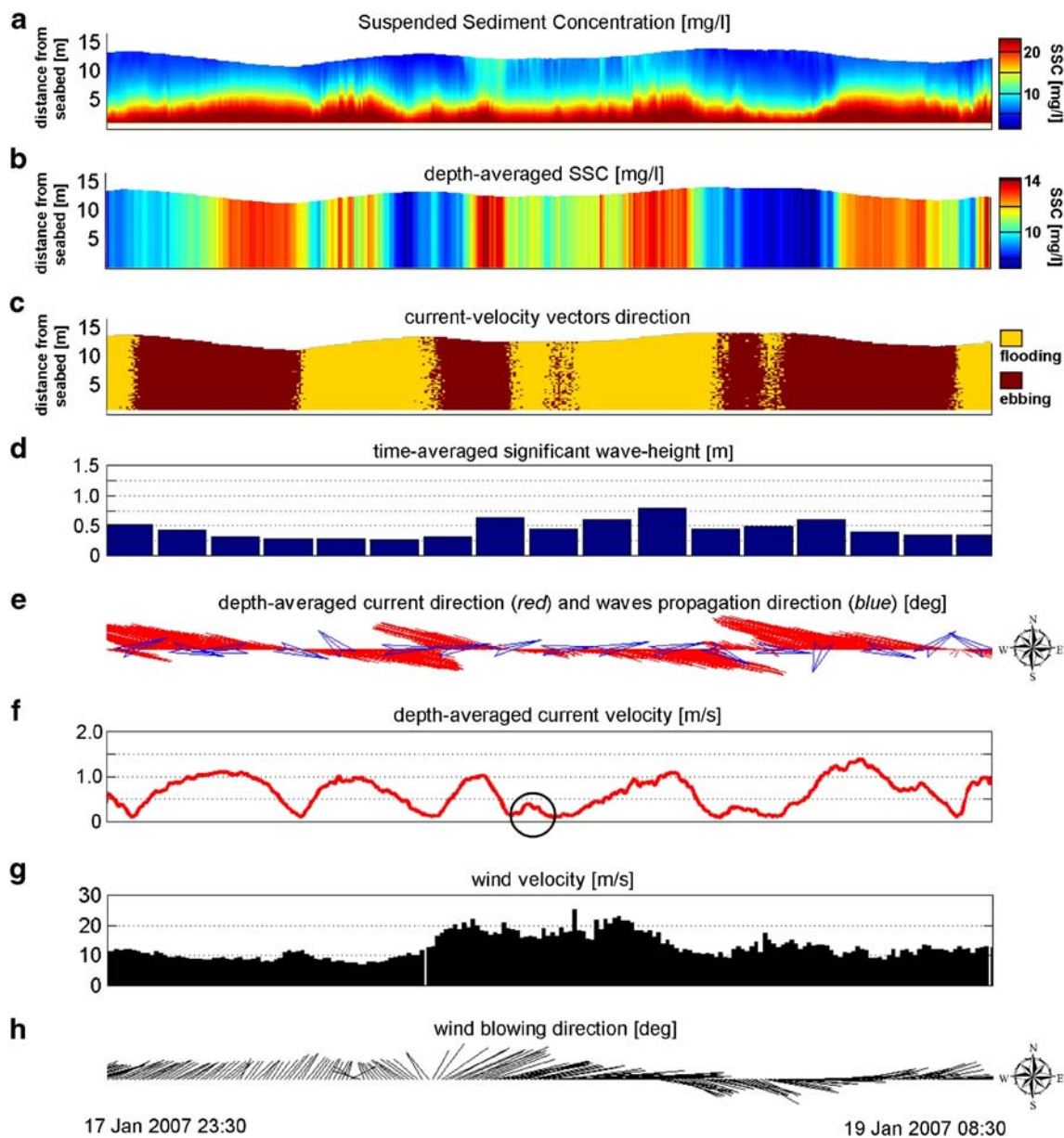


**Fig. 8** Storm surge “Kyrill” on 18th January 2007 shown as **a** backscatter-related SSC; **b** depth-averaged backscatter-related SSC; **c** water flow direction; **d** significant wave height; **e** depth-integrated

flow direction and wave propagation direction; **f** depth-averaged flow velocity; **g** wind velocity; and **h** wind blowing direction. The storm took place during the ebb phase

significantly longer in duration and characterised by flow speeds reaching almost  $1.5 \text{ m s}^{-1}$ , i.e. values up to 50% higher than usual (Fig. 8f). The remobilisation of sediment was less pronounced than during storm “Britta”.

### 5 Discussion

The results of this study, which are based on measurements on different time scales, confirm the general trend of ebb-

dominated transport of suspended sediment during low energy conditions in the Spiekeroog back-barrier tidal system. Net transport takes place predominantly in the lower part of the water column, as was previously demonstrated by field data as well as model reconstructions (e.g. Pejrup 1988; Santamarina Cuneo and Flemming, 2000; Brink-Spalink 2005; Stanev et al. 2003a, b, 2006; Lettman et al. 2009). One should be aware that SSC values differ significantly depending on the calibration methods and adopted measurement strategies. The measured con-

centration values used in this study, which are based on in situ pump samples and LISST optical transmission, were mainly recorded during relatively low energy conditions. This explains the good correspondence with other data sets collected during similar weather conditions. The good fit between in situ SSC derived from LISST and time-averaged pump samples shows that maximum SSCs of up to almost  $60 \text{ mg l}^{-1}$  are the rule in this area under such conditions (see Table 1), a conclusion supported by the findings of Santamarina Cuneo and Flemming (2000), which were related to similar energy situations. Although the concentrations of sandy material recorded under higher energy conditions differ significantly in the two studies, the discrepancy between absolute values is of secondary importance when discussing the interaction of waves, tidal currents and sediment transport. Unfortunately, it was not possible to track sediment transport in the lower 1 m of the water column where, as demonstrated in many studies, most of the remobilisation takes place. We observed no significant increase of the ADCP backscatter intensity of sample bins during high-energy events, but the distribution of high-intensity bins in the ADCP profile shows that large clouds of suspended sediment were lifted towards the water surface.

On different time scales, substantial variations in SSCs and floc sizes were observed. Thus, concentrations during low-energy conditions varied between  $10$  and  $30 \text{ mg l}^{-1}$ , and the maxima in SSC were slightly phase-shifted to 30–40 min after slack water. The mean floc sizes over a tidal cycle varied from nearly  $180 \text{ }\mu\text{m}$  at maximum current to almost  $380 \text{ }\mu\text{m}$  shortly after slack high water. The range of floc sizes is limited by parameters such as current velocity, turbulence intensity, SSC, tidal period and the amount of organic matter (e.g. Edelvang and Austen 1997; Fettweis et al. 2006). The variation in floc size was mostly controlled by the flocculation/floc break-up behaviour of the suspended material. This explains why in our case floc size is mainly correlated with current velocity.

As shown by the example during calm-weather conditions with minor influence of wind and waves, SSC varies over spring–neap cycles. Highest SSCs are observed near the seabed during spring tide. This is due to the higher current velocities in the tidal basin, which can generate more turbulence. During such conditions, the turbulent kinetic energy increases by a factor of 10, and this, in turn, allows high remobilisation rates (Ridderinkhof et al. 2000; Bartholomä et al. 2008; Karle 2008). In the longer term, one would expect a significant seasonal signal in SSCs. The in situ SSC data from LISST and from pump samples, however, reveal neither tidal-phase- nor season-related changes (see Table 1). The seasonal signal is also not clearly reflected in the mean floc size of our data-sets, but the maximum floc size was only observed in summer. This

may be explained by a higher organic input into the system (Jördel et al. 2004; Lunau et al. 2006).

When the wave height increases, the remobilisation rate increases subsequently. Dependent on the wind and wave direction, the net sediment transport direction is very variable in contrast to the net transport of water (Ridderinkhof et al. 2000). The results of modelled suspended sediment transport for the East Frisian part of the Wadden Sea (Stanev et al. 2006) show that the concentration of suspended particulate matter (SPM) in the water column is relatively high in the presence of high water levels and/or strong wind waves. This especially applies to cases with high wind waves, which result in increased bottom shear stress, higher erosion and hence higher SSCs (Stanev et al. 2006). Above all, this has been assumed to be the case during short-term extreme events such as the storm in November 2006 (Britta) and January 2007 (Kyrill), where higher SSCs were indeed registered throughout the water column. While a significant wave height of around  $0.4 \text{ m}$  (Krögel and Flemming 1998) appears to be representative for fair weather conditions, significant wave heights of almost  $1.5 \text{ m}$  were measured at the pile during the storms. Such wave heights are also twice as large as those measured under usual high-energy conditions during winter seasons (Krögel & Flemming, 1998).

During the storm event “Tilo” on 9th November 2007, maximum SSCs exceeding  $120 \text{ mg l}^{-1}$  were measured in the water column of Otzum Inlet (Badewien et al. 2009). Concentrations of up to  $140 \text{ mg l}^{-1}$  during strong winds were reported by Santamarina Cuneo (2000), but these included the sand fraction. Such high values are probably caused by the higher turbulence in the water column. Exceptionally during severe storms, the entire water column is characterised by high backscatter values, suggesting a homogeneous distribution of high SSC. During such events the remobilisation phenomena can be compared to the tidal flats situation where any increase in energy generates higher remobilisation of deposited material. This documents the importance of waves in shallow water with turbulence affecting the entire water column. In deeper channels, by contrast, wave-generated turbulence is largest near the surface where it adds noise to the backscatter intensity produced by scatterers in the water column. This aspect requires attention in the future because the ambient noise adversely affects the accuracy of the conversion of backscatter intensity into SSC.

During extreme events, the common situation observed on tidal flats appears to be transferred to the tidal channels. During both storm events, higher SSC values were registered throughout the entire water column. However, duration and impact intensity are strictly dependent on how the tidal phase and wind/wave direction interact. The coastal damage caused by the two storm events varied

along the East Frisian coast line. During the November 2006 storm “Britta”, the combination of flood phase and wind together with waves from northwestern direction accelerated the flood current dramatically, eventually resulting in a storm surge with water levels exceeding those of the disastrous storm event of 1962. The unprecedented water volume drained rapidly during the subsequent, substantially prolonged ebb phase that was accompanied by a rapid change in wind direction, followed by a distinct net export of suspended material. Only one ebb phase later, the system had almost returned to “normal”.

The second storm “Kyrill”, which struck the coast in January 2007, showed a similar rapid change in wind speed and direction but with other basic parameters. During this event, winds from southwesterly directions generated waves, which propagated against the ebb flow at that time. During the storm maximum, the wind direction rotated more than 40° towards the northwest. In this case, the next upcoming flood phase was also prolonged in a similar manner as during the “Britta” event. However, in contrast to the storm surge of November 2006, the January 2007 storm shortened the duration of two successive ebb phases by almost 70% of the “normal” ebb flow durations. This means that, even if at that time more suspended matter was present in the water column, only a small amount would have been exported during the strongly compressed ebb phases, which, in addition, had greatly reduced flow velocities. This implies that increased turbulence in the water column associated with increased wave heights does not automatically mean more export of material. It is now quite clear that, during extreme events when wind and wave impact operate in conjunction over short time scales only, transport budgets can change in both directions.

## 6 Conclusions

This paper presents time series of stationary and mobile measurements of SSC, in situ particle sizes, wind, wave and current data on different time scales. The data were collected from mobile and stationary platforms in the tidal catchment area of the mesotidal back-barrier tidal flat of Spiekeroog Island on the East Frisian coast in the Southern North Sea. The following conclusions can be drawn from this study:

- Over individual tidal cycles, depth-averaged SSCs derived from ADCP can reach up to 20 mg l<sup>-1</sup>, but water sample data yield values larger than 60 mg l<sup>-1</sup>, keeping in mind that ADCP-based SSCs are likely to be underestimated. The mean particle size is tide-dependent and varies between 180 μm at maximum flow and 380 μm shortly after slack water. The variation in size results from differences in aggregation

and disaggregation behaviour of individual particles, which, in turn, is controlled by the current velocity. On a time scale of weeks, SSC increases during the spring tide period.

- Contrary to expectations, a seasonal signal in the SSC data was not detected. This is in contradiction to observations reported for other case studies in the North Sea region. Floc size, by contrast, follows the seasonal signal, reaching twice the size during the organically enriched spring–summer period.
- During low-energy conditions, the ebb-dominated system suggests net export, although SSCs are generally low. During high-energy conditions, when waves also affect deeper channels, the export of material due to extreme events is mainly controlled by the interference of wind/wave and tidal phase. In such cases, the basic ebb dominance can be temporarily counteracted or even completely eliminated by flood-dominant conditions. Sudden dynamic changes of wind force and/or direction can squeeze the ebb phase duration by over 70%, resulting in distinctly reduced or even neutralised export of suspended material. The higher backscatter intensity does not automatically imply higher concentrations of SSC over the entire water column and therefore does not automatically imply higher export rates.

**Acknowledgements** The authors would like to thank all the helpers in the field; especially named are technicians Axel Braun, Maik Wilsenack and the Jade Service diving team for their engagement in servicing the underwater deployment at the pile. The captain and crew of RV Senckenberg made an excellent job during all the cruises. The reviewers are acknowledged for helpful criticism, comments and suggestions. This project was funded by Deutsche Forschungsgemeinschaft as part of the DFG Research Group “BioGeoChemistry of Tidal Flats” at the University of Oldenburg.

## References

- Agrawal YC, Pottsmith HC (2000) Instruments for particle size and settling velocity observations in sediment transport. *Mar Geol* 168:89–114. doi:10.1016/S0025-3227(00) 00044-X
- Agrawal YC, Whitmore A, Mikkelsen OA, Pottsmith HC (2008) Light-scattering by random shaped particles and consequences on measuring suspended sediments by laser diffraction. *J Geophys Res* 113:C04023. doi:10.1029/2007JC004403
- Badewien TH, Zimmer E, Bartholomä A, Reuter R (2009) Towards continuous long-term measurements of suspended particulate matter (SPM) in turbid coastal waters. *Ocean Dynamics, Special Issue - WATT*. doi:10.1007/s10236-009-0183-8
- Bartholdy J, Aagard T (2001) Storm surge effects on a back-barrier tidal flat of the Danish Wadden Sea. *Geo Mar Lett* 20:113–141
- Bartholomä A (1993) Zeitliche Variabilität und räumliche Inhomogenität in den Substrateigenschaften und der Zoobenthosbesiedlung im Umfeld von Miesmuschelbänken. *D. Hydrodynamik. Berichte Senckenberg am Meer* 93(1):117–123

- Bartholomä A, Flemming BW (2007) Progressive grain-size sorting along an intertidal energy gradient. In: Flemming BW, Hartmann D (eds) From particle size to sediment dynamics. Proceeding of a Workshop, 15–18 April 2004, Hanse Institute for Advanced Study, Delmenhorst (Germany). *Sediment Geol (Spec. Issue)* 202: 464–472. doi:10.1016/j.sedgeo.2007.03.010
- Bartholomä A, Schrottke K, Winter C (2008) Sand wave dynamics: Surfing between assumptions and facts. In: Parsons D, Garlan T, Best J (eds) *Marine and River Dune Dynamics*, pp 17–24
- Brink-Spalink G (2005) Untersuchung der Dynamik des Sedimenttransportes im Ostfriesischen Wattenmeer mit einem numerischen Modell. PhD thesis, ICBM Carl-von-Ossietzky University Oldenburg, p 117
- Chang TS, Joerdel O, Flemming BW, Bartholomä A (2006) Importance of flocs and aggregates in muddy sediment dynamics and seasonal sediment turnover in a back-barrier tidal basin of the East Frisian Wadden Sea (southern North Sea). *Mar Geol* 235:49–61. doi:10.1016/j.margeo.2006.10.004
- Chang TS, Flemming BW, Bartholomä A (2007) Distinction between sortable silts and aggregated particles in muddy intertidal sediments of the southern North Sea. *Sediment Geol* 202:453–463. doi:10.1016/j.sedgeo.2007.03.009
- Davis RA Jr, Flemming B (1991) Time-series study of mesoscale tidal bedforms, Martens Plate, Wadden Sea, Germany. In: Smith DG, Reinson GE, Zaitlin BA, Rahmani RA (eds) *Clastic Tidal Sedimentology*, Canadian Society of Petroleum Geologists. *Memoir* 16:275–282
- de Haas H, Eisma D (1993) Suspended sediment transport in the Dollard Estuary. *Neth J Sea Res* 31:37–42. doi:10.1016/0077-7579(93) 90014-J
- Eldvang K, Austen I (1997) The temporal variation of flocs and fecal pellets in a tidal channel. *Estuar Coast Shelf Sci* 44(3):361–367. doi:10.1006/ecss.1996.0149
- Fettweis M (2008) Uncertainty of excess density and settling velocity of mud flocs derived from in situ measurements. *Estuar Coast Shelf Sci* 78:426–436. doi:10.1016/j.ecss.2008.01.007
- Fettweis M, Francken F, Pison V, Van den Eynde D (2006) Suspended particulate matter dynamics and aggregate sizes in a high turbidity area. *Mar Geol* 235(1–4):63–74. doi:10.1016/j.margeo.2006.10.005
- Fitzgerald DM, Penland S (1987) Backbarrier dynamics of the East Frisian Islands. *J Sediment Res* 57(4):746–754
- Flemming BW (2002) Effects of climate and human interventions on the evolution of the Wadden Sea depositional system (southern North Sea). In: Wefer G, Berger W, Behre K-E, Jansen E (eds) *Climate development and history of the North Atlantic Realm*. Springer, Berlin, pp 399–413
- Flemming BW, Ziegler K (1995) High-resolution grain size distribution patterns and textural trends in the backbarrier tidal flats of Spiekeroog Island (southern North Sea). *Senckenb Marit* 26:1–24
- Fugate D, Friedrichs C (2002) Determining concentration and fall velocity of estuarine particle populations using adv, obs and listt. *Cont Shelf Res* 22:1867–1886. doi:10.1016/S0278-4343(02) 00043-2
- Hayes M (1979) Barrier island morphology as a function of tidal and wave regime. In: Leatherman SP (ed) *Barrier Islands from the Gulf of St. Lawrence to the Gulf of Mexico*. Academic, New York, pp 1–29
- Hoitink A, Hoekstra P (2005) Observations of suspended sediment from ADCP and OBS measurements in a mud-dominated environment. *Coast Eng* 52(2):103–118. doi:10.1016/j.coastaleng.2004.09.005
- Holdaway G, Thorne P, Flatt D, Jones S, Prandle D (1999) Comparison between adcp and transmissometer measurements of suspended sediment concentration. *Cont Shelf Res* 19:421–441. doi:10.1016/S0278-4343(98) 00097-1
- Jördel O, Flemming BW, Bartholomä A (2004) Flocculation, flocc-breakup and grain-size composition of suspended sediments in tidal waters of the southern North Sea. In: Flemming BW, Hartmann D, Delafontaine MT (eds) From particle size to sediment dynamics. International Workshop, 15–18 April 2004, Hanse Institute for Advanced Study, Delmenhorst, Germany. *Research Center Terramare Reports* 13:86–89
- Karle M (2008) Turbulenzgesteuertes Erosionsverhalten von Wattedimenten am Beispiel des Rückseitenwatts der Insel Spiekeroog—Untersuchungen mit hochauflösender Sonartechnik, Elect Pub, University Marburg, p 108
- Kawanisi K, Yokosi S (1997) Characteristics of suspended sediment and turbulence in a tidal boundary layer. *Cont Shelf Res* 17(8):859–875. doi:10.1016/S0278-4343(96) 00066-0
- Krögel F, Flemming BW (1998) Evidence for temperature-adjusted sediment distributions in the back-barrier tidal flats of the East Frisian Wadden Sea (southern North Sea). In: Alexander CR, Davis RA, Henry VJ (eds) *Tidalites: processes and products*. SEPM Special Publication 61:31–41
- Lettman KA, Wolff J-O, Badewien TH (2009) Modeling the impact of wind and waves on suspended particulate matter fluxes in the East Frisian Wadden Sea (southern North Sea). *Ocean Dyn*. doi:10.1007/s10236-009-0194-5
- Lumborg U, Pejrup M (2005) Modelling of cohesive sediment transport in a tidal lagoon—an annual budget. *Mar Geol* 218:1–16. doi:10.1016/j.margeo.2005.03.015
- Lunau M, Lemke A, Dellwig O, Simon M (2006) Physical and biogeochemical controls of microaggregate dynamics in a tidally affected coastal ecosystem. *Limnol Oceanogr* 51(2): 847–859
- Mai S, Bartholomä A (2000) The missing mud flats of the Wadden Sea: a reconstruction of sediments and accommodation space lost in the wake of land reclamation. In: Flemming BW, Delafontaine MT, Liebezeit G (eds) *Muddy coast dynamics and resource management*. Elsevier Science, Amsterdam, pp 257–272
- Merckelbach LM (2006) A model for high-frequency acoustic Doppler current profiler backscatter from suspended sediment in strong currents. *Cont Shelf Res* 26:1316–1335. doi:10.1016/j.csr.2006.04.009
- Nikora V, Goring D (2002) Fluctuations of suspended sediment concentration and turbulent sediment fluxes in an open-channel flow. *J Hydrol Eng* 128(2):214–224. doi:10.1061/(ASCE) 0733-9429(2002) 128:2(214)
- Pejrup M (1988) Suspended sediment transport across a tidal flat. *Mar Geol* 82(3–4):187–198. doi:10.1016/0025-3227(88) 90140-5
- Reuter R, Badewien TH, Bartholomä A, Braun A, Lübben A, Rullkötter J (2009) A hydrographic time-series station in the Wadden Sea (southern North Sea). *Ocean Dyn* (this issue)
- Ridderinkhof H, van der Ham R, van der Lee W (2000) Temporal variations in concentration and transport of suspended sediments in a channel-flat system in the Ems–Dollard estuary. *Cont Shelf Res* 20(12–13):1479–1493. doi:10.1016/S0278-4343(00) 00033-9
- Santamarina Cuneo P (2000) Fluxes of suspended particulate matter through a tidal inlet of the East Frisian Wadden Sea (southern North Sea). Reports, Fachbereich Geowissenschaften, University Bremen, p 100
- Santamarina Cuneo P, Flemming BW (2000) Quantifying concentration and flux of suspended particulate matter through a tidal inlet of the East Frisian Wadden Sea by acoustic Doppler current profiling. In: Flemming BW, Delafontaine MT, Liebezeit G (eds) *Muddy coast dynamics and resource management*. Elsevier Science, Amsterdam, pp 39–51
- Stanev EV, Flöser G, Wolff J-O (2003a) Dynamical control on water exchanges between tidal basins and the open ocean. A case study

- for the East Frisian Wadden Sea. *Ocean Dyn* 53:146–165. doi:[10.1007/s10236-003-0029-8](https://doi.org/10.1007/s10236-003-0029-8)
- Stanev EV, Wolff J-O, Burchard H, Bolding K, Flöser G (2003b) On the circulation in the East Frisian Wadden Sea: numerical modeling and data analysis. *Ocean Dyn* 53:27–51. doi:[10.1007/s10236-002-0022-7](https://doi.org/10.1007/s10236-002-0022-7)
- Stanev EV, Wolff J-O, Brink-Spalink G (2006) On the sensitivity of the sedimentary system in the East Frisian Wadden Sea to sea-level rise and wave-induced bed shear stress. *Ocean Dyn* 56:266–283. doi:[10.1007/s10236-006-0061-6](https://doi.org/10.1007/s10236-006-0061-6)
- Stanev EV, Flemming BW, Bartholomä A, Staneva JV, Wolff J-O (2007) Vertical circulation in shallow tidal inlets and back-barrier basins. *Cont Shelf Res* 27:798–831. doi:[10.1016/j.csr.2006.11.019](https://doi.org/10.1016/j.csr.2006.11.019)
- Talke S, Stacey M (2008) Suspended sediment fluxes at an intertidal flat: the shifting influence of wave, wind, tidal and freshwater forcing. *Cont Shelf Res* 28:710–725
- Trevethan M, Chanson H, Takeuchi M (2007) Continuous high-frequency turbulence and suspended sediment concentration measurements in an upper estuary. *Estuar Coast Shelf Sci* 73:341–350. doi:[10.1016/j.ecss.2007.01.014](https://doi.org/10.1016/j.ecss.2007.01.014)
- Voulgaris G, Meyers ST (2004) Temporal variability of hydrodynamics, sediment concentration and sediment settling in a tidal creek. *Cont Shelf Res* 24:1659–1683. doi:[10.1016/j.csr.2004.05.006](https://doi.org/10.1016/j.csr.2004.05.006)
- Xu W (2000) Mass physical sediment properties and trends in a Wadden Sea tidal basin. *Berichte, Fachbereich Geowissenschaften. Univ Bremen* 157:127